ELSEVIER

Thermochimica Acta 334 (1999) 107–113

thermochimica acta

www.elsevier.com/locate/tca

Study of thermal decomposition of $FeC_2O_4 \cdot 2H_2O$ under hydrogen

Valérie Carles, Pierre Alphonse*, Philippe Tailhades, Abel Rousset

Laboratoire de Chimie des Matériaux Inorganiques et Energétiques, ESA CNRS 5070, 118 route de Narbonne, 31062 Toulouse Cedex 04, France

Received 23 November 1998; accepted 20 May 1999

Abstract

Thermal decomposition of $FeC_2O_4 \cdot 2H_2O$ under Ar, H_2/Ar mixture and H_2, was studied by thermogravimetric measurements with quantitative analysis of the gaseous products by both mass spectrometry and infrared spectroscopy. The oxalate decomposition appears rather independent of the H_2 partial pressure, giving a mixture of Fe_3O_4, α-Fe, CO and CO_2. But, in fact, when the H_2 partial pressure is high enough, CO produced by the decomposition is hydrogenated in CH_4 (and in less extent into C_2H_6) according to a Fischer–Tropsch reaction catalyzed by α-Fe. This reaction is also accompanied by the formation of cementite (θ-Fe_3C). Upon further heating, Fe_3O_4 reduction to metallic iron occurs followed by decomposition of iron carbide also into α-Fe. The effect of experimental parameters on the reaction process is discussed.

Keywords: Thermal decomposition; Thermogravimetric measurements; Fischer–Tropsch reaction; Ferrous oxalate

1. Introduction

Thermal decomposition of oxalates has been extensively studied [1] essentially because it is an easy and powerful method for the preparation of small particles of metals, metallic alloys, metallic oxides and mixed metallic oxides. Among these numerous works, many have been devoted to the study of decomposition of ferrous oxalate under inert or oxidizing atmosphere (air, O_2) [2–8], but only a few can be found on the decomposition of ferrous oxalate under H_2 [9–12]. Moreover these papers either do not deal with the various gas–solid reactions that take place during the reduction process, or if they do, some of these interpretations appear in disagreement with our experimental results. Hence the aim of this work is to report the detailed and quantitative analysis of the various gas–solid reactions that occur during the decomposition of ferrous oxalate under H_2 and actually to discuss how the reaction process depends on the choice of the reaction parameters (partial pressure of H_2, O_2 and H_2O, heating rate, volumetric flow rate).

2. Experimental

2.1. Materials

$FeCl_2$, $4H_2O$ was dissolved in an hydroalcoholic solution (ethanol 90 vol%–water 10 vol%) containing a small amount of hydrochloric acid (to prevent Fe^{2+} oxidation). The ferrous oxalate was precipitated at 20°C from this hydroalcoholic solution with ethanol

*Corresponding author. Tel.: +33-05-61-62-85; fax: +33-05-61-55-61-63.

0040-6031/99/$ – see front matter
PII: S0040-6031(99)00133-1

solution of oxalate acid [13]. After 5 min of stirring, the precipitate was separated by filtration, washed with demineralized water and dried at 90°C. The average length of the acicular oxalate particles is about 0.3 μm. Ar, H_2/Ar mixture and H_2 gas of high purity grade (>99.995%) were used.

2.2. Characterization

The products were analyzed by X-ray powder diffraction with a Siemens diffractometer using Cu K_α radiation. Surface areas were measured by nitrogen adsorption (B.E.T method) using a Micrometrics Flowsorb 2300. Scanning electron microscopy was carried out with a JEOL JSM 6400 (with an accelerating voltage of 20 kV).

2.3. Thermal analyses of oxalate decomposition

These analyses were performed in a vertical quartz glass reactor build around a Cahn D200 electrobalance (accuracy 10^{-6} g). The oxalate sample was loaded into an alumina pan; this pan is hanged to a Nichrome suspension wire attached to the balance beam. A tubular furnace, driven by a temperature programmer, allows to linearly raise the sample temperature. An accurately control of the sample temperature is given by a K type thermocouple installed very close to the sample pan. The balance is connected to a rotary vacuum pump and a side arm of the vacuum takeoff tube is connected to a Pirani gauge. Another side arm provides an entrance for the inlet gas (H_2, 10% H_2 in Ar or Ar). The bottom of the reactor is fitted to a mass flow meter and the outlet gas is further analyzed by Infra-Red (IR) spectrometry (with a low volume gas cell fitted to a Nicolet 510P spectrometer) and Mass Spectrometry (MS, Leybold Inficon Transpector H200M).

The sample was first outgassed under primary vacuum (5 Pa) at room temperature during 30 min. Then the apparatus was filled with the required gas. During the experiment the changes of sample temperature, sample weight, volumetric flow rate, gas composition (followed by IR and MS spectra) are recorded every 30 s.

The sample mass was in the range 0.02–0.04 g, the volumetric flow rate in the range 0.04–0.08 l min^{-1} and the heating rate in the range 1–5°C min^{-1}.

3. Results and discussion

3.1. Thermogravimetric analyses

The TGA curves (Fig. 1) of ferrous oxalate decomposition, recorded under various atmospheres, show that the dehydration and decomposition steps are well separated (by almost 200°C). The dehydration step corresponds to a relative weight loss of 20.0% which indicates that our starting material was the di-hydrate oxalate $FeC_2O_4{\cdot}2H_2O$. In pure H_2, the dehydration occurs at a slightly lower temperature (about 10°C) than in 10% H_2–90% Ar and in pure Ar.

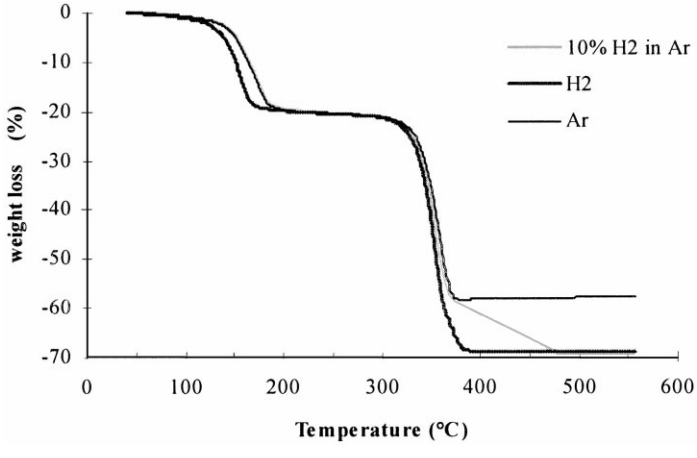

Fig. 1. TGA of $FeC_2O_4{\cdot}2H_2O$ decomposition – heating rate = 2°C min^{-1}.

The decomposition step appears almost independent of the H_2 partial pressure. Under pure H_2, the total weight loss is 69.0% which is in accordance with the formation of metallic iron; indeed X-ray diffraction pattern analysis confirms that the solid product at the end of the experiment is only α-Fe. Under Ar, as soon as the decomposition ended (380°C), the weight loss is 58.2%; then a slow weight increase is noticed and above 500°C the weight loss is close to the expected one for the formation of Fe_3O_4 (57.5%). Indeed X-ray diffraction pattern analysis confirms that the final solid product is magnetite. So, the product formed after the first step of the decomposition undergoes oxidation although the partial pressure of O_2 in Ar is very low (<20 ppm). Under 10% H_2–90% Ar mixture, the reaction leads to metallic iron, as in pure H_2, but via an intermediate product similar to the one formed under Ar.

The maximum temperature (T_m) at which dehydration and decomposition take place is dependent of the heating rate (β) and the apparent activation energy (E_a) can be calculated, for the two reaction steps, from some experimentally collected pairs of T_m and β values [14]. Since we have worked with a differential reactor (with low fractional conversion), the value of E_a can be deduced from the slope of the line $\ln(\beta/T_m^2) = f(1/T_m)$.

Apparent activation energy of the two steps was found independent of the H_2 partial pressure (Table 1). Hence it can be assumed that H_2 does not play a direct role in the first stage of decomposition process.

Table 1
Apparent activation energy (kJ/mol)

	Dehydration	Decomposition
10% H_2 in Ar	86	152
100% H_2	85	152

3.2. Quantitative analysis of gaseous products by IR and MS

3.2.1. Decomposition under AR

The detected gaseous products are CO and CO_2 (Fig. 2). Thus the anhydrous ferrous oxalate breaks down according to the reaction:

$$FeC_2O_4 \rightarrow FeO + CO + CO_2 \quad (1)$$

But FeO is not stable under these conditions [15] and a dismutation occurs giving a mixture of Fe and Fe_3O_4:

$$FeO \rightarrow Fe_3O_4 + Fe \quad (2)$$

As we have shown above with TGA, the O_2 partial pressure was high enough to slowly oxidize the iron and to finally give the magnetite Fe_3O_4.

Reaction (1) implies that equivalent amount of CO and CO_2 might be detected, but CO concentration in gaseous phase was always found lower than the CO_2

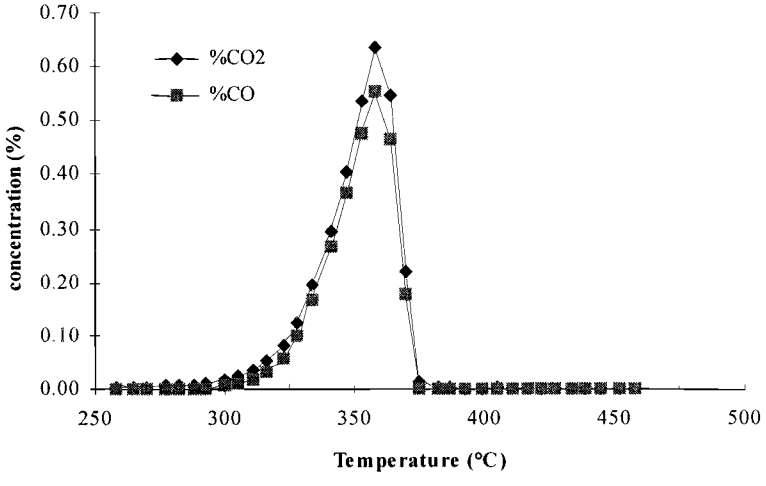

Fig. 2. Decomposition of FeC_2O_4 under Ar – sample mass = 0.04 g; flow rate = 0.06 l min^{-1}; heating rate = 2°C min^{-1}.

one. This can be due to CO oxidation by O_2, catalyzed by Fe_3O_4:

$$CO + 1/2O_2 \rightarrow CO_2 \quad (3)$$

3.2.2. Decomposition under H_2

The reaction appears quite different than under Ar because at the beginning of the decomposition: (i) equivalent amount of CH_4 and H_2O are formed; (ii) CO is not detected (Fig. 3). Actually this can be explained by a decomposition according to reaction (1), giving CO, CO_2 and FeO, followed by dismutation of FeO according to reaction (2). Under H_2, metallic iron produced by reaction (2) could act as catalyst for CO hydrogenation according to a Fischer–Tropsch reaction:

$$CO + 3H_2 \rightarrow CH_4 + H_2O \quad (4)$$

This reaction explains why equivalent amount of CH_4 and H_2O are formed at the beginning of oxalate decomposition. But α-Fe is not stable and is quickly converted by the action of CO/H_2 into iron carbide θ-Fe_3C (cementite); the possible reactions are (5) and (6):

$$3Fe + 2CO \rightarrow Fe_3C + CO_2 \quad (5)$$

$$3Fe + CO + H_2 \rightarrow Fe_3C + H_2O \quad (6)$$

In fact, at low CO concentration, reaction (5) could probably be neglected since carbide formation has not been detected without H_2. On the other hand X-ray diffraction pattern analysis of the semi-decomposed solid has only shown the presence of θ-Fe_3C without other iron carbide (such as Fe_5C_2 or Fe_7C_3) probably because the C/Fe ratio was too low in our experiments. It can be noticed that reaction (6) explains why H_2O partial pressure becomes larger than the CH_4 one from 330°C.

But it is well known that in Fischer–Tropsch reaction the initial high activity of iron catalyst falls off as it becomes progressively carbided [16]. Moreover the increasing amount of CO_2 induces also a deactivation caused by the covering of the metallic surface by oxygen atoms (generated by the dissociation of CO_2). Hence, less and less CO reacts according to the reaction (4) and a large increase of CO partial pressure associated with a decrease of the rate of CH_4 formation are observed from 340°C.

On the other hand, C_2H_6 is formed from 330°C. This is an additional evidence of a Fischer–Tropsch reaction because an increase in CO partial pressure raises the CO/H_2 ratio and thus changes the selectivity of the reaction toward the formation of C_2 hydrocarbons.

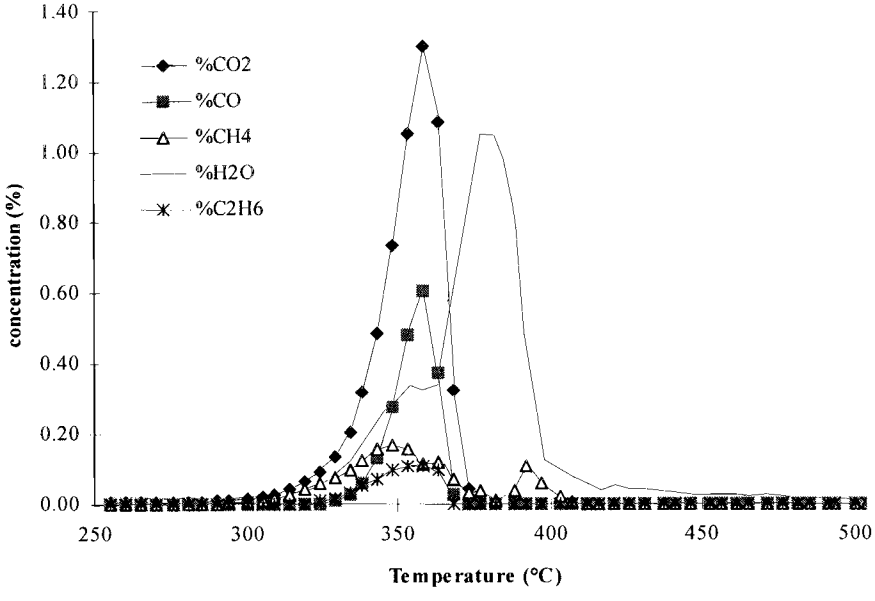

Fig. 3. Decomposition of FeC_2O_4 under H_2 – sample mass = 0.03 g; flow rate = 0.04 l min^{-1}; heating rate = 2°C min^{-1}.

Above 360°C, the H_2O partial pressure significantly increases because of Fe_3O_4 reduction to α-Fe according to:

$$Fe_3O_4 + 4H_2 \rightarrow 3Fe + 4H_2O \quad (7)$$

Above 380°C, another CH_4 emission occurs, linked to the decomposition of iron carbide:

$$Fe_3C + 2H_2 \rightarrow 3Fe + CH_4 \quad (8)$$

3.2.3. Decomposition under 10% H_2 in Ar mixture

The beginning of the reaction seems quite similar to the decomposition under Ar since only CO and CO_2 are detected (Fig. 4). But above 320°C, equivalent amount of CH_4 and H_2O are formed and further a little amount of C_2H_6 is also detected. Hence, in the far less extent than under pure H_2, we can guess the occurrence of a Fischer–Tropsch reaction with formation of small amount of Fe_3C. Above 370°C, the strong increase in H_2O concentration corresponds to the beginning of the reduction of Fe_3O_4 by H_2. It can be noticed here that H_2O formation takes place in two steps in agreement with the two successive reductions of Fe_3O_4:

$$Fe_3O_4 + H_2 \rightarrow 3FeO + H_2O \quad (9)$$

$$FeO + H_2 \rightarrow Fe + H_2O \quad (10)$$

Emission of CO was detected above 400°C without formation of CO_2 or hydrocarbons. This could be explained by the reaction:

$$Fe_3C + \tfrac{1}{2}O_2 \rightarrow 3Fe + CO \quad (11)$$

The methanization of iron carbide (reaction 8) probably could not occur because the H_2 partial pressure is too low.

3.3. Discussion about the effect of experimental parameters

The operating variables having an effect on the reaction process are mainly: the partial pressure of H_2, H_2O and O_2, the sample mass to volumetric flow rate ratio and the heating rate.

The H_2 partial pressure acts on both metal carbide formation and metal particle growth. First, we have shown that a low H_2 partial pressure decreases the extent of carbide formation. The main drawback of iron carbide is the formation of two kind of metal particles resulting either from reduction of Fe_3O_4 (reaction (7)) or from the decomposition of iron carbide (reaction (8)). Hence carbide formation must be avoided if either unimodal distribution of metallic

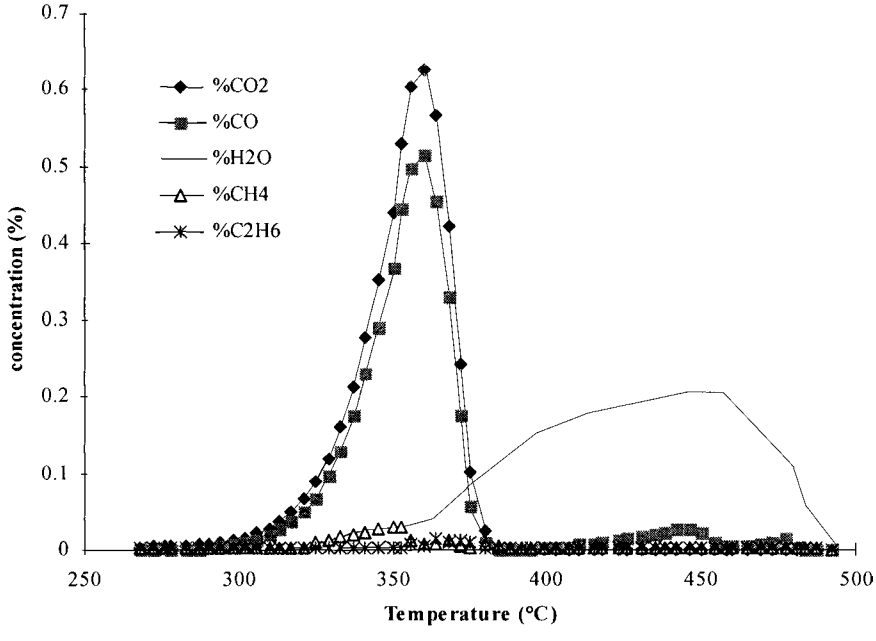

Fig. 4. Decomposition of FeC_2O_4 under 10% H_2 in Ar – sample mass = 0.04 g; flow rate = 0.06 l min^{-1}; heating rate = 2°C min^{-1}.

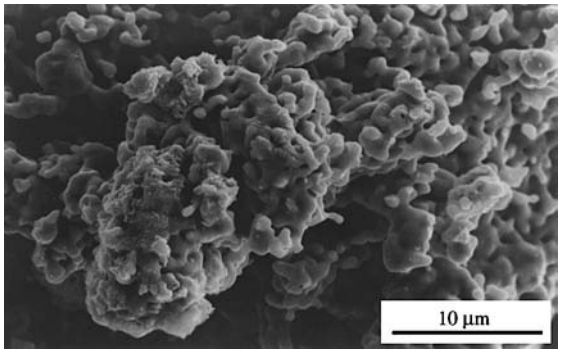

Fig. 5. SEM micrograph of metal particles synthetized by decomposition of $FeC_2O_4{\cdot}2H_2O$ under H_2 sample mass = 0.4 g; flow rate = 0.2 l min^{-1}; heating rate = 2°C min^{-1}.

particle or pure metallic alloy is required. Indeed, it will be difficult to obtain a pure metallic alloy because the kinetic of carbide formation will probably not be the same for each metal leading to multiphased material.

On the other hand, H_2 partial pressure also acts on metal particle growth. Indeed the more the H_2 partial pressure the less the temperature at which the reaction is achieved. So, for a given temperature, metallic crystallites will be smaller at low H_2 pressure. The influence of H_2 partial pressure on the average size and size distribution of metallic iron crystallites is well illustrated comparing the SEM micrographs of Fig. 5 (pure H_2, average size about 1.3 μm) and Fig. 6 (10% H_2 in Ar, average size about 0.6 μm).

The O_2 partial pressure has an effect on the CO/CO_2 ratio through reaction (3), catalyzed by Fe_3O_4. Since the formation of iron carbide is directly linked to the CO partial pressure (reaction (6)), the O_2 partial pressure also acts on the amount of carbide formed.

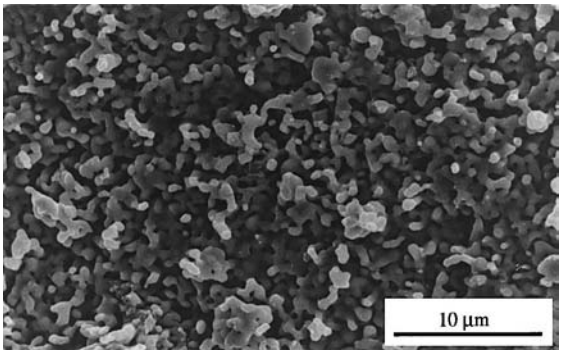

Fig. 6. SEM micrograph of metal particles synthetized by decomposition of $FeC_2O_4{\cdot}2H_2O$ under 10% H_2 in Ar sample mass = 0.4 g; flow rate = 0.2 l min^{-1}; heating rate = 2°C min^{-1}.

In this work we have not studied the effect of the partial pressure of H_2O. However we can assume that this parameter could modify the reaction process because the ''water–gas shift reaction'', $CO + H_2O \rightarrow CO_2 + H_2$, is catalyzed by Fe_3O_4.

The mass/flow rate ratio mainly modifies the partial pressure of the CO and CO_2 gaseous products. In the above experiments, this ratio was rather low, in the range 0.25–1.0 g l^{-1} min. Then, the CO and CO_2 concentrations were at the most 1% for a heating rate of 1°C min^{-1} or 2°C min^{-1}. These conditions, initially selected for working with low fractional conversion (differential reactor), minimize the carbide formation (less than 10% under pure H_2). But it seems obvious that for larger mass/flow rate ratios this proportion will strongly increase.

For a given gas flow rate, the heating rate acts on the reaction rate, thus modifying the partial pressure of CO and CO_2 as the mass/flow rate ratio does. But, this parameter has also an effect on the crystallization state of metal particles.

Finally, we think that the understanding of the different reactions occurring during the oxalate decomposition process allows to control these reactions by acting on the suitable experimental parameters. We are now studying how to tune the operating variables in order to synthesize metal particles with a required size and size distribution.

4. Conclusion

The oxalate decomposition appears rather independent of the H_2 partial pressure, giving first a mixture of FeO, Fe, CO and CO_2. However FeO is unstable and is converted into α-Fe and Fe_3O_4. When the partial pressure of H_2 is high enough, the CO produced by the decomposition is hydrogenated into CH_4 (and to a lesser extent into C_2H_6) according to a Fischer–Tropsch reaction catalyzed by metallic Fe. This reaction is also accompanied by the formation of cementite (θ-Fe_3C). Upon further heating, α-Fe is formed first from Fe_3O_4 reduction and then from iron carbide decomposition.

References

[1] D. Dollimore, Thermochimica Acta 117 (1987) 331.
[2] J. Robin, J. Bénard, C.R. Acad. Sci. (France) 232 (1951) 1830.
[3] J. Robin, Bull. Soc. Chim. Fr., Mém. (1953) 1078.
[4] A. Boullé, J.L. Dorémieux, C.R. Acad. Sci. (France) 248 (1959) 2211.
[5] J.L. Dorémieux, A. Boullé, C.R. Acad. Sci. (France) 250 (1960) 3184.
[6] D. Dollimore, D. Nicholson, J. Chem. Soc. (1962) 960.
[7] D. Dollimore, D.L. Griffiths, D. Nicholson, J. Chem. Soc. (1963) 2617.
[8] D. Broadbent, D. Dollimore, J. Dollimore, J. Chem. Soc. (1967) 451.
[9] P. Brissaud, J.L. Dorémieux, P. Dugleux, C.R. Acad. Sc. Paris, Série C 272 (1971) 222.
[10] S. Caric, L. Marinkov, J. Slivka, Phys. Stat. Sol. (a) 13 (1975) 263.
[11] J.L. Dorémieux, Colloques Internationaux du CNRS 201 (1972) 631.
[12] F. Li, Y. Kong, D. Xue, Phys. Stat. Sol. (a) 148 (1995) 129.
[13] CNRS, P. Tailhades, M. Gougeon, Ch. Bonino-Salvaing, A. Rousset, P. Mollard, Eu. Pat. 86905854.5 (1987).
[14] H.E. Kissinger, J. Res. National Bureau of Standards 57(4) (1956) 217.
[15] G. Chaudron, Ann. Chim. (France) 9 (1921) 221.
[16] M. Pijolat, M. Perrichon, M. Primet, P. Bussière, J. Mol. Catal. 17 (1982) 367.